

RFID Thermal Monitoring Sheet (R-TMS) for Skin Temperature Measurements during Superficial Microwave Hyperthermia Treatment

Francesco Lestini
*Pervasive Electromagnetics Lab
Civil Engineering and Computer
Science Engineering Dept.
University of Rome Tor Vergata
Rome, Italy
f.lestini97@gmail.com*

Nicoletta Panunzio, *IEEE Member*
*Pervasive Electromagnetics Lab
Civil Engineering and Computer
Science Engineering Dept.
University of Rome Tor Vergata
Rome, Italy
nicoletta.panunzio@uniroma2.it*

Gaetano Marrocco, *IEEE Member*
*Pervasive Electromagnetics Lab
Civil Engineering and Computer
Science Engineering Dept.
University of Rome Tor Vergata
Rome, Italy
gaetano.marrocco@uniroma2.it*

Cecilia Occhiuzzi, *IEEE Member*
*Pervasive Electromagnetics Lab
Civil Engineering and Computer
Science Engineering Dept.
University of Rome Tor Vergata
Rome, Italy
cecilia.occhiuzzi@uniroma2.it*

Abstract—Hyperthermia is a widely used anti-cancer treatment that exploits the interactions between high-power electromagnetic fields and the human tissues to locally release a great amount of power in the underlying tissue regions. The electromagnetic source is generally outside the body, in close proximity to the skin. Thus, dangerous hotspots may occur within the skin, and hence continuous monitoring of the superficial temperature distribution is required throughout the treatment. Current Thermal Monitoring Sheets (TMSs), that are grids of many temperature sensors, have some limitations in terms of poor spatial resolution and high thermal conduction errors. Passive Ultra High Frequency (UHF) Radio Frequency Identification (RFID) devices could offer an attractive alternative thanks to their wireless nature, low-invasiveness, and demonstrated good on-skin performance, especially for temperature monitoring. The preliminary design of an RFID-based Thermal Monitoring Sheet (R-TMS) is presented in this paper as a planar array of circular loop antennas with temperature-sensing-oriented RFID ICs. Both sensing and electromagnetic requirements of the R-TMS are addressed by means of numerical simulations. It proved capable of transmitting the collected temperature data with a remarkable spatial resolution, yet without interfering with the effectiveness of the hyperthermia treatment nor inducing unwanted hotspots over the skin.

Keywords—RFID, Frequency Selective Surface, skin temperature, hyperthermia, sensors array

I. INTRODUCTION

Hyperthermia is a long-established adjuvant local anti-cancer treatment. It uses temperatures exceeding the physi-

ologically optimal level (typically 40-43°C for approximately one hour) to function as a necrotic actuator, radiosensitizer, or chemosensitizer [1]. In particular, electromagnetic heating techniques apply a high frequency alternating sinusoidal field, generated by one or more antennas, to locally release a great amount of power in the region to be treated without damaging the surrounding tissues. These EM fields cause dielectric heating up to the desired therapeutic temperature by molecular dipole rotation/polarization/vibration in the MHz range (i.e., 434 MHz) [1]. To properly transfer the energy into body tissues, a water bolus is usually interposed between the antenna and the skin. This water bolus can be simultaneously used for skin cooling when treating deep-seated tumors, or for heating in the case of superficial tumor locations.

One of the main risks for the patient during treatment is the onset of possible superficial hotspots that can cause damages and thermal toxicity [1]. Hence, adequate monitoring of skin temperature throughout the treatment is fundamental. A planar and body-conformable grid of temperature sensors can be distributed over the skin for this purpose, provided that it meets the technical requirements outlined by the European Society for Hyperthermic Oncology (ESHO) [2]. First of all, the Thermal Monitoring Sheet (TMS) should not interfere with the effectiveness of the treatment, meaning that it should not shield the EM field penetration into the body. Then, to achieve an accurate and reliable spatial thermal pattern of the skin region, the involved thermal sensors must have accuracy $\leq 0.2^\circ\text{C}$, resolution $\leq 0.1^\circ\text{C}$, and stability $\leq 0.1^\circ\text{C}/\text{hr}$. The spatial temperature resolution should be at least $20 \times 20 \text{ mm}$, with thermal conduction errors $\leq 10 \text{ mm}$ produced by the

The work was developed in the framework of the Dual-Skin project, funded by Italian Ministry of University and Research (FISR 2020 COVID, Ref. FISR2020IP 00227).

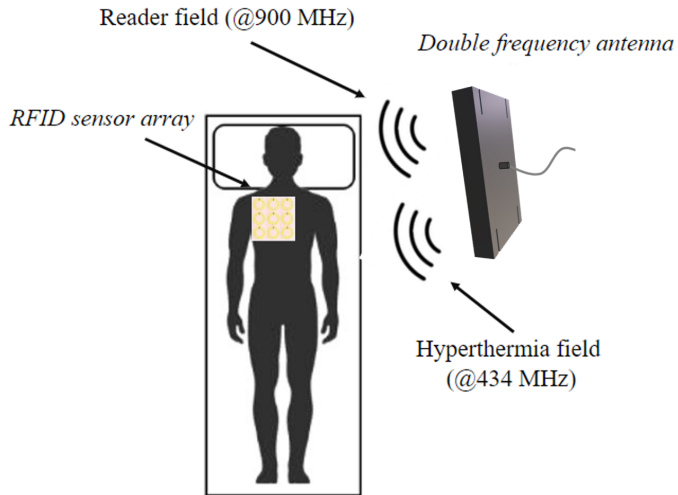


Fig. 1. Concept of the RFID-based Thermal Monitoring Sheet (R-TMS).

conductive materials constituting the sensors. Moreover, a short placement time is required to put the TMS in place over the patient as the maximum effectiveness of hyperthermia is achieved when it is performed immediately after standard anti-cancer treatments [3].

Sensors arrays can be made of thermocouples, thermistors, or fiber optic probes [4]. Currently, the best solution [5] involves a maximum of 56 thermocouples spread over a thin silicone layer. Besides the good accuracy ($0.06^{\circ}C$), temperature resolution ($0.0156^{\circ}C$), and stability ($< 0.01^{\circ}C/h$), this TMS is expensive and features a sub-optimal spatial resolution ($20 \times 25 mm$) and high thermal conduction errors due to the long cables that carry the temperature signals from the thermocouples to the acquisition system.

Flexible and wireless *Epidermal Electronics* may offer an attractive alternative to improve the spatial resolution of the probes and to minimize the interference with the treatment. In particular, epidermal and battery-less Ultra High Frequency (UHF) Radio Frequency IDentification (RFID) devices [6] have notably increased their real-world applicability in recent years for the wireless, low-cost, and non-invasive measurement of skin parameters, temperature above all [7], [8]. These devices rely on backscattering communication to transmit the data and involve simple integrated circuits (ICs) for both communication and temperature sensing [9]. Hence, passive UHF RFID sensor devices can be notably miniaturized while maintaining good communication performance [10], so that an array of these sensors could provide a high-resolution temperature spatial map. Moreover, the absence of long wires over the skin could greatly reduce the thermal conduction errors and the interference with the treatment.

This paper presents the preliminary design of a UHF RFID sensors array to function as an RFID-based Thermal Monitoring Sheet (R-TMS) for the monitoring of skin temperature over the body region involved in a hyperthermia treatment (Fig. 1). The aim is to provide a wireless and low-cost solution with a

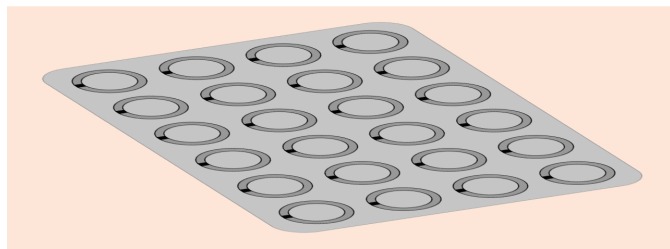


Fig. 2. Concept of on-skin R-TMS made of 6×4 circular radiating elements over a thin layer of biosilicone.

high spatial temperature resolution and practical ease of use. To fulfill the additional requirements deriving from the use of RF sensors (Section II), the RFID Thermal Monitoring Sheet (R-TMS) is modeled and numerically simulated (Section III). The size of the elementary sensor antenna is optimized by a parametric analysis in terms of both the transmission performance at 434 MHz and the data communication performance at 900 MHz. Finally, the Specific Absorption Rate (SAR) in the muscle and within the skin is evaluated at 434 MHz (Section IV) to verify that the presence of the sensors array is safe for the patient and does not affect the hyperthermia treatment.

II. RFID THERMAL MONITORING SHEET (R-TMS)

The proposed RFID-based Thermal Monitoring Sheet (R-TMS) is conceived to be made as a planar repetition of an elementary radiating element, deposited over a thin layer of biocompatible silicone (Fig. 2). Each antenna will be provided with an RFID IC with an embedded solid-state temperature sensor (i.e., the Axzon Magnus-S3 IC [9] that has already been thoroughly involved in skin temperature¹ monitoring applications [7]). In this way, the introduction of expensive and bulky external sensors is avoided, allowing the radiating elements to be arranged as closely as possible to meet the high-resolution requirement.

An envisaged application scenario of the R-TMS is sketched in Fig. 1. The UHF reader antenna that powers the sensors and collects the backscattered data could be integrated within the same handpiece of the hyperthermia applicator. Two radiating antennas working at different frequencies (i.e., 434 MHz and 900 MHz) could cohabit in the applicator, or a single dual-frequency antenna could be fabricated.

The use of RF sensors, however, adds additional requirements that must be verified to assess the feasibility of such system. (i) The array must be *invisible* (i.e., minimal induced current over the R-TMS) at the working frequency of the hyperthermia applicator (i.e., 434 MHz). This will allow to achieve an adequate value of SAR in the muscle and to avoid hotspots over the skin. (ii) The array must be able to collect the external power (i.e., maximum induced current over the R-TMS) and to transmit back the temperature data to an external reader in the UHF band (i.e., 900 MHz).

¹Operation range: $-40^{\circ}C \leq T \leq 85^{\circ}C$; resolution: $0.13^{\circ}C$ [9]. Accuracy and precision for body temperature measurement: $0.2^{\circ}C$ [11].

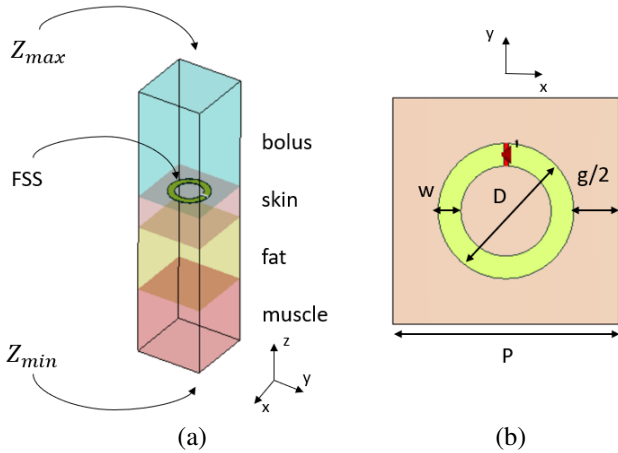


Fig. 3. (a) Stratified numerical model of the unit cell, with indication of Floquet ports Z_{max} and Z_{min} . (b) Circular loop radiating element. The parameters are: D = loop external diameter, w = loop trace width, g = elements gap, and $P = g + D$ periodicity of the unit cell.

TABLE I
DIELECTRIC PROPERTIES OF TISSUES AND WATER BOLUS [12].

| | ϵ | σ [S/m] | Thickness [mm] |
|--------|------------|----------------|-------------------|
| Bolus | 80 | 0.04 | 17 ^(a) |
| Skin | 46.1 | 0.702 | 5 |
| Fat | 11.6 | 0.082 | 10 |
| Muscle | 56.9 | 0.81 | 10 ^(b) |

(a) Water bolus thickness was chosen accordingly to [13].

(b) Muscle thickness was chosen as the SAR is normalized with respect to its maximum value at this depth [13], [14].

III. DESIGN OF THE R-TMS SENSORS ARRAY

To meet the need for a double-frequency response, the R-TMS can be designed by means of the Frequency Selective Surfaces (FSSs) [15], modeled by Floquet's theory [16]. Indeed, the FSSs are 2D periodic arrays of metallic elements (or apertures) that exhibit both stop-band (i.e., reflection of incident wave) and pass-band (i.e., transparency w.r.t. incident wave) behaviors when excited by electromagnetic waves at different frequencies.

To design the sensors array, the *periodic structures* template of CST Microwave Studio 2018 was used to perform numerical simulations. It allows to simulate a single unit cell, but considering its repetition to infinity along both x and y directions (orthogonal to the propagation direction).

A. Unit Cell

The unit cell (Fig. 3.a) was made by a rectangular layered phantom (i.e., muscle, fat, skin) covered by the water bolus. Dielectric properties are in Table I. Two Floquet ports (i.e., Z_{max} and Z_{min}) were set at the upper and lower boundaries of the computational domain, respectively, to evaluate the scattering parameters between them. In particular, the Z_{max} port is set over the bolus, at the position of the transmission antenna, whereas the Z_{min} port is set 1 cm deep in the muscle,

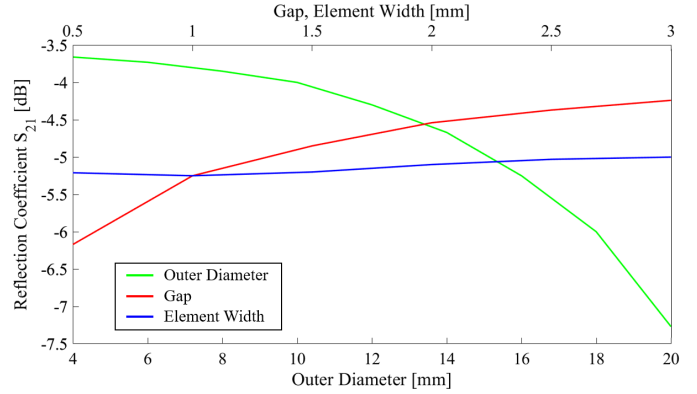


Fig. 4. Transmission coefficient as a function of geometric parameters.

where the treatment effectiveness is conventionally evaluated in terms of Specific Absorption Rate (SAR). The transmission coefficient S_{21} of the phantom alone (i.e., in the absence of the FSS) was evaluated at the hyperthermia working frequency of 434 MHz to derive the maximum achievable value, that is -3.64 dB.

A circular aluminum loop (Fig. 3.b) was chosen as the on-skin radiating element of the FSS due to its realization simplicity, easy parametrization, and stability with respect to the plane wave's angle of incidence [17]. The starting values of the unit cell parameters were chosen as $P = 18$ mm, $D = 16$ mm, $g = 2$ mm, and $w = 1$ mm, as they allow for a spatial temperature resolution of 18×18 mm, which fulfills the ESHO requirements and outperforms the state-of-the-art. Furthermore, the periodicity $P = 18$ mm ensures that no higher-order Floquet modes will be excited in the structure. Indeed, in order to work in the *no-grating-lobes regime*, the periodicity of the structure has to be lower than half wavelength [17], which is approximately 42 mm at (900 MHz) in this work. Hence, only the two fundamental propagating Floquet modes TE_{00} and TM_{00} will be excited in the chosen structure.

B. Parametric Analysis

In order to fulfill the electromagnetic requirements of the RFID sensors array, parametric analyses were performed at both hyperthermia frequency of 434 MHz and data interrogation frequency of 900 MHz.

1) *Transmission at 434 MHz*: The parametric analysis at 434 MHz aimed at obtaining a value of the transmission coefficient S_{21} of the structure, evaluated at Z_{min} (i.e., 1 cm deep in the muscle), that is as close as possible to the maximum achievable value of -3.64 dB derived above in the absence of the FSS. It followed that, by increasing the diameter D or by reducing the width w and the elements gap g , the transmission coefficient is reduced, and vice versa (Fig. 4). In particular, the largest effect is played by the diameter D (i.e., the smaller, the better), whereas the loop trace width w and the element gap g have a minimal effect on the transmission coefficient. But, to minimize the metal traces on the skin, which are the main cause of hotspots, a narrow width is preferable.

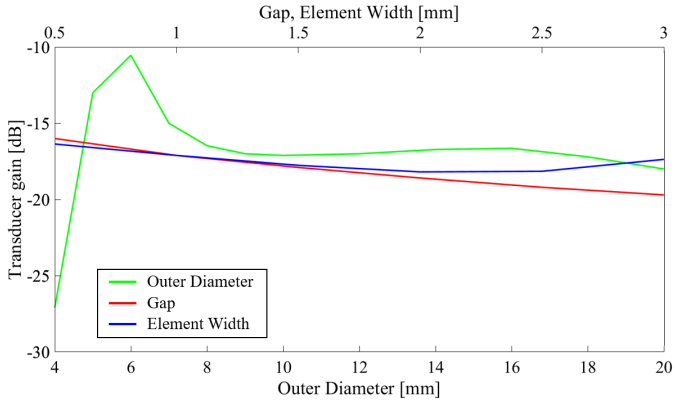


Fig. 5. Transducer gain as a function of geometric parameters.

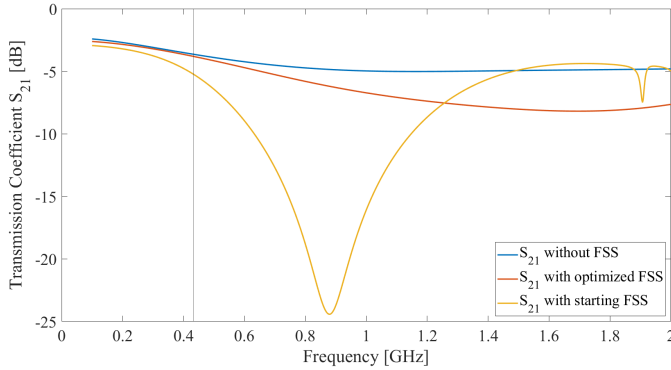


Fig. 6. Transmission coefficient of the structure with and without the FSS.

Therefore, the following parameter values were chosen for the next analysis: $D = 4 \text{ mm}$, $g = 2 \text{ mm}$, and $w = 1 \text{ mm}$. The corresponding transmission coefficient is $S_{21} = -3.67 \text{ dB}$, which is fully comparable with that in the absence of the FSS. This means that, with this choice of size, the presence of the loop antenna would not alter the treatment effectiveness.

2) *Communication at 900 MHz*: The chosen 434 MHz configuration was then evaluated in terms of the communication performance at 900 MHz. As the communication occurs in the near-field, the transducer gain G_T [18] was chosen as the metrics to be maximized. To compute the calculation, the input impedance value of the Axzon Magnus-S3 RFID IC [9] was exploited.

A new parametric analysis revealed that, by increasing the diameter D of the loop, the transducer gain increases at first and then decreases to an asymptotic value of about -16 dB (Fig. 5). This trend is in contrast to the results of the previous analysis at 434 MHz. Therefore, a trade-off was required to meet both specifications. The final parameters were chosen as $D = 6 \text{ mm}$, $g = 1 \text{ mm}$, and $w = 1 \text{ mm}$. In particular, the loop trace width w was kept equal to 1 mm due to its minimal effect on the transducer gain, whereas the diameter D was increased to the value of 6 mm for which the transducer gain is maximum. The periodicity P increased accordingly to 7 mm . With this choice of parameters, the transducer gain is -8.1 dB , which is a good value to ensure communication, and

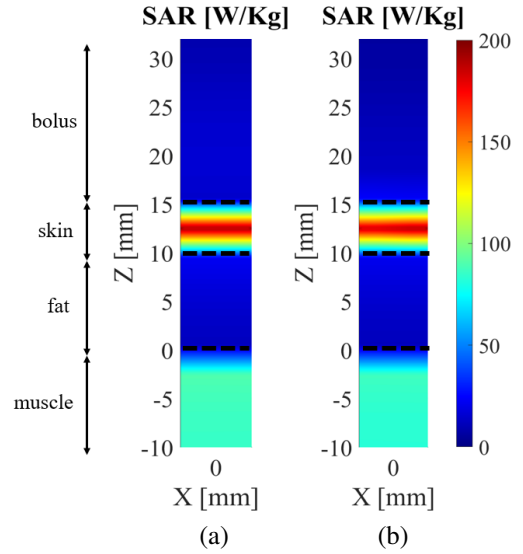


Fig. 7. SAR distribution over $y = 6.5 \text{ mm}$ plane in case of y -polarized plane wave excitation. (a) Reference unit cell without FSS. (b) Unit cell with optimized FSS.

the transmission coefficient is -3.82 dB (Fig. 6), only slightly lower than before. Moreover, it is worth noticing that, the trend of the transmission coefficient of the optimized FSS is notably improved with respect to the starting unit cell.

IV. EVALUATION OF SAR

By exploiting the optimized FSS radiating element, a preliminary evaluation of the Specific Absorption Rate (SAR) distribution inside the structure was performed at 434 MHz with a twofold purpose: (i) to verify that the hyperthermia treatment is not altered by the presence of the R-TMS, and (ii) to verify that no hotspots are generated on the skin. The SAR distribution inside the phantom in the absence of the FSS was taken as the reference model (Fig. 7.a). Fig. 7.b, instead, shows the SAR distribution in the presence of the FSS. Two SAR values are evaluated and compared: the value at 1 cm deep in the muscle (i.e., $z = -10 \text{ mm}$), and the maximum value reached within the skin layer.

The optimized R-TMS does not reduce the effectiveness of the hyperthermia treatment as, by considering a typical input power of 100 W supplied to the applicator, the SAR value in the muscle is approximately 61 W/Kg , which is fully comparable to the required value of 60 W/kg [19]. Furthermore, there is no relevant increase of SAR on the skin, which reaches 160 W/Kg with respect to 155 W/Kg in the absence of the FSS.

V. CONCLUSION

The paper presented the design of an RFID Thermal Monitoring Sheet (R-TMS), that is an epidermal array of UHF RFID temperature sensors that can be used for skin temperature monitoring during superficial hyperthermia treatments. The thorough parametric analysis led to the definition of a configuration that fulfills all the technical specifications by ESHO

[2]. In particular, the spatial resolution is notably improved up to $7 \times 7 \text{ mm}$ (w.r.t. the minimum requirement of $20 \times 20 \text{ mm}$).

The main strength of the proposed prototype is that it enables the *wireless* transmission of the temperature data, hence it is minimally invasive for the patient and easy to put in place by the clinical operator since wired probes are avoided. The R-TMS was numerically tested at both hyperthermia frequency (434 MHz) and data interrogation frequency (900 MHz). It proved able to properly transmit the temperature data (i.e., transducer gain of -8.1 dB with a commercially available IC) but without interfering with the hyperthermia treatment (i.e., SAR of 61 W/kg in the muscle w.r.t. the minimum requirement of 60 W/kg [19]). Moreover, the R-TMS seems safe for the patient as hotspots within the skin do not occur.

Experimental evaluations at both frequencies as well as temperature tests in a controlled mock-up are in progress. Results will be shown at the conference.

REFERENCES

- [1] H. P. Kok, "Heating technology for malignant tumors: a review," *Int J Hyperthermia*, vol. 37, no. 1, pp. 711–741, January 2020.
- [2] J. Crezee, M. Schmidt, D. Marder, U. Lamprecht, M. Ehmann, J. Nadobny, J. Hartmann, N. Lomax, S. Abdel-Rahman, S. Curto, A. Bakker, M. D. Hurwitz, C. J. Diederich, P. R. Stauffer, and G. C. Van Rhooon, "Quality assurance guidelines for superficial hyperthermia clinical trials : II. Technical requirements for heating devices," *Strahlenther Onkol*, vol. 193, no. 5, pp. 351–366, May 2017.
- [3] C. van Leeuwen, A. Oei, R. Cate, N. Franken, A. Bel, L. Stalpers, H. Crezee, and H. Kok, "Measurement and analysis of the impact of time-interval, temperature and radiation dose on tumour cell survival and its application in thermoradiotherapy plan evaluation," *International Journal of Hyperthermia*, vol. 34, pp. 1–26, April 2017.
- [4] A. Bakker, R. Zweije, H. Kok, M. Kolff, H. Bongard, M. Schmidt, G. van Tienhoven, and H. Crezee, "Clinical Feasibility of a High-Resolution Thermal Monitoring Sheet for Superficial Hyperthermia in Breast Cancer Patients," *Cancers*, vol. 12, p. 3644, December 2020.
- [5] A. Bakker, R. Zweije, G. van Tienhoven, H. P. Kok, J. Sijbrands, D. van den Bongard, C. Rasch, and H. Crezee, "Two high-resolution thermal monitoring sheets for clinical superficial hyperthermia," *Phys Med Biol*, June 2020.
- [6] S. Amendola, C. Occhiuzzi, C. Miozzi, S. Nappi, F. Amato, F. Camera, and G. Marrocco, *UHF epidermal sensors: Technology and applications*, November 2020, pp. 133–161.
- [7] N. Panunzio and G. Marrocco, "SECOND SKIN Project: BioIntegrated Wireless Sensors for the Epidermal Monitoring and Restoring of Sensorial Injuries," in *2021 IEEE International Conference on RFID Technology and Applications (RFID-TA)*, October 2021, pp. 173–176.
- [8] C. Occhiuzzi, S. Parrrella, F. Camera, S. Nappi, and G. Marrocco, "RFID-Based Dual-Chip Epidermal Sensing Platform for Human Skin Monitoring," *IEEE Sensors Journal*, vol. 21, no. 4, pp. 5359–5367, October 2021.
- [9] Axzon, "RFM3300-E Magnus-S3 M3E passive sensor IC," <https://axzon.com/rfm3300-e-magnus-s3-m3e-passive-sensor-ic/>, September 2021.
- [10] F. Camera, C. Miozzi, F. Amato, C. Occhiuzzi, and G. Marrocco, "Experimental Assessment of Wireless Monitoring of Axilla Temperature by Means of Epidermal Battery-Less RFID Sensors," *IEEE Sensors Letters*, vol. 4, no. 11, pp. 1–4, November 2020.
- [11] F. Camera and G. Marrocco, "Electromagnetic-Based Correction of Bio-Integrated RFID Sensors for Reliable Skin Temperature Monitoring," *IEEE Sensors Journal*, vol. 21, no. 1, pp. 421–429, August 2021.
- [12] IT²IS Foundation, "Tissue properties database summary," 2021. [Online]. Available: <https://itis.swiss/virtual-population/tissue-properties/database/database-summary/>
- [13] H. Petra Kok, D. Correia, M. De Greef, G. Van Stam, A. Bel, and J. Crezee, "SAR deposition by curved CFMA-434 applicators for superficial hyperthermia: Measurements and simulations," *Int J Hyperthermia*, vol. 26, no. 2, pp. 171–184, 2010.
- [14] H. P. Kok, M. De Greef, D. Correia, P. J. Vording, G. Van Stam, E. A. Gelvich, A. Bel, and J. Crezee, "FDTD simulations to assess the performance of CFMA-434 applicators for superficial hyperthermia," *Int J Hyperthermia*, vol. 25, no. 6, pp. 462–476, August 2009.
- [15] F. Capolino, *Theory and Phenomena of Metamaterials (1st ed.)*. CRC Press, October 2009.
- [16] A. K. Bhattacharyya, *Phased Array Antennas : Floquet Analysis, Synthesis, BFNs and Active Array Systems*. Wiley-Interscience, March 2006.
- [17] B. A. Munk, *Frequency Selective Surfaces: Theory and Design*. New York: Wiley, 2000.
- [18] S. J. Orfanidis, *Electromagnetic Waves and Antennas*, 2016, Available: <https://www.ece.rutgers.edu/orfanidi/ewa/>.
- [19] P. Wust, H. Stahl, J. Loffel, M. Seebass, H. Riess, and R. Felix, "Clinical, physiological and anatomical determinants for radiofrequency hyperthermia," *International Journal of Hyperthermia*, vol. 11, no. 2, pp. 151–167, April 1995.